

Experimental investigation of the extraction of solitons at the initial stage of the soliton formation process

M. Bello-Jiménez,^{1,*} E. A. Kuzin,¹ O. Pottiez,² B. Ibarra-Escamilla,¹ A. Flores-Rosas,¹
and M. Durán-Sánchez³

¹Instituto Nacional de Astrofísica, Óptica y Electrónica, Luis Enrique Erro N. 1, Departamento de Óptica, Puebla, Pue 72000, México

²Centro de Investigaciones en Óptica, Lomas del Bosque N. 115, Departamento de Fibras Ópticas, León, Gto 37150, México

³Universidad Tecnológica de Puebla, Antiguo camino a la resurrección No. 1002-A, Zona industrial, Puebla, Pue 72300, México

*mabello@inaoep.mx

Abstract: We demonstrate the extraction of a single soliton from a bunch of solitons generated by the pulse breakup effect. The bunch of solitons was generated in a 500-m fiber pumped by 25-ps pulses. For the extraction of single soliton from the bunch we use a nonlinear optical loop mirror (NOLM). At its output we detected a pulse with full width at half-maximum (FWHM) of 0.99 ps whose autocorrelation trace corresponds to that of a soliton. Our results demonstrate that the suggested method can be useful for soliton generation, and also for investigations of the initial stage of the soliton formation process.

©2009 Optical Society of America

OCIS codes: (060.4370) Nonlinear optics, fibers; (060.5530) Pulse propagation and temporal solitons.

References and links

1. F. Mollenauer, R. H. Stolen, and J. P. Gordon, "Experimental observation of picosecond pulse narrowing and soliton in optical fiber," *Phys. Rev. Lett.* **45**(13), 1095–1098 (1980).
2. L. F. Mollenauer, R. H. Stolen, J. P. Gordon, and W. J. Tomlinson, "Extreme picosecond pulse narrowing by means of soliton effect in single-mode optical fibers," *Opt. Lett.* **8**(5), 289–291 (1983).
3. A. S. Gouveia-Neto, A. S. L. Gomes, and J. R. Taylor, "Generation of 33-fsec pulses at 132 μm through a high-order soliton effect in a single-mode optical fiber," *Opt. Lett.* **12**(6), 395–397 (1987).
4. J. P. Gordon, "Theory of the soliton self-frequency shift," *Opt. Lett.* **11**(10), 662–664 (1986).
5. F. M. Mitschke, and L. F. Mollenauer, "Discovery of the soliton self-frequency shift," *Opt. Lett.* **11**(10), 659–661 (1986).
6. K. Tai, A. Hasegawa, and N. Bekki, "Fission of optical solitons induced by stimulated Raman effect," *Opt. Lett.* **13**(5), 392–394 (1988).
7. P. Beaud, W. Hodel, B. Zysset, and H. P. Weber, "Ultrashort pulse propagation, pulse breakup, and fundamental soliton formation in a single-mode optical fiber," *IEEE J. Quantum Electron.* **QE-23**(11), 1938–1946 (1987).
8. S. R. Friberg, and K. W. DeLong, "Breakup of bound higher-order solitons," *Opt. Lett.* **17**(14), 979–981 (1992).
9. D. Krylov, L. Leng, K. Bergman, J. C. Bronski, and J. N. Kutz, "Observation of the breakup of a prechirped N-soliton in an optical fiber," *Opt. Lett.* **24**(17), 1191–1193 (1999).
10. M. G. Banaee, and J. F. Young, "High-order soliton breakup and soliton self-frequency shifts in a microstructured optical fiber," *J. Opt. Soc. Am. B* **23**(7), 1484–1489 (2006).
11. C.-J. Rosenberg, D. Anderson, M. Desaix, P. Johannisson, and M. Lisak, "Evolution of optical pulses toward wave breaking in highly nonlinear fibers," *Opt. Commun.* **273**(1), 272–277 (2007).
12. P. Podlipensky, P. Szarniak, N. Y. Joly, and P. S. Russell, "Anomalous pulse breakup in small-core photonic crystal fibers," *J. Opt. Soc. Am. B* **25**(12), 2049–2056 (2008).
13. Hasegawa, and W. F. Brinkman, "Tunable coherent IR and FIR sources utilizing modulational instability," *IEEE J. Quantum Electron.* **QE-16**, 694–697 (1980).
14. A. S. Gouveia-Neto, M. E. Faldon, and J. R. Taylor, "Raman amplification of modulational instability and solitary-wave formation," *Opt. Lett.* **13**(11), 1029–1031 (1988).
15. M. N. Islam, G. Sucha, I. Bar-Joseph, M. Wegener, J. P. Gordon, and D. S. Chemla, "Femtosecond distributed soliton spectrum in fibers," *J. Opt. Soc. Am. B* **6**(6), 1149–1158 (1989).

16. S. Mendoza-Vazquez, E. A. Kuzin, S. Chavez-Cerda, B. Ibarra-Escamilla, J. Gutierrez-Gutierrez, J. W. Haus, and R. Rojas-Laguna, "Pulse breakup and Raman-shifted solitons in a standard fiber with subnanosecond pumping in the presence of noise," *J. Opt. Soc. Am. B* **23**(11), 2336–2341 (2006).
17. J. K. Ranka, R. S. Windeler, and A. J. Stentz, "Visible continuum generation in air-silica microstructure optical fibers with anomalous dispersion at 800 nm," *Opt. Lett.* **25**(1), 25–27 (2000).
18. T. A. Birks, W. J. Wadsworth, and P. St. J. Russell, "Supercontinuum generation in tapered fibers," *Opt. Lett.* **25**(19), 1415–1417 (2000).
19. J. M. Dudley, L. Provino, N. Grossard, H. Maillotte, R. S. Windeler, B. J. Eggleton, and S. Coen, "Supercontinuum generation in air-silica microstructured fibers with nanosecond and femtosecond pulse pumping," *J. Opt. Soc. Am. B* **19**(4), 765–771 (2002).
20. A. K. Abeeluck, and C. Headley, "Continuous-wave pumping in the anomalous- and normal-dispersion regimes of nonlinear fibers for supercontinuum generation," *Opt. Lett.* **30**(1), 61–63 (2005).
21. K. J. Blow, N. J. Doran, and B. K. Nayar, "Experimental demonstration of optical soliton switching in an all-fiber nonlinear Sagnac interferometer," *Opt. Lett.* **14**(14), 754–756 (1989).
22. M. N. Islam, E. R. Sunderman, R. H. Stolen, W. Pleibel, and J. R. Simpson, "Soliton switching in a fiber nonlinear loop mirror," *Opt. Lett.* **14**(15), 811–813 (1989).
23. K. Smith, N. J. Doran, and P. G. J. Wigley, "Pulse shaping, compression, and pedestal suppression employing a nonlinear-optical loop mirror," *Opt. Lett.* **15**(22), 1294–1296 (1990).
24. M. Bello-Jiménez, E. A. Kuzin, O. Pottiez, B. Ibarra-Escamilla, A. Flores-Rosas, and M. Durán-Sánchez, "Soliton extraction from a bunch of solitons resulting from pulse breakup by using a nonlinear optical loop mirror," *J. Opt. Soc. Am. B* **26**(7), 1456–1462 (2009).
25. B. Ibarra-Escamilla, E. A. Kuzin, P. Zaca-Morán, R. Grajales-Coutiño, F. Mendez-Martinez, O. Pottiez, R. Rojas-Laguna, and J. W. Haus, "Experimental investigation of the nonlinear optical loop mirror with twisted fiber and birefringence bias," *Opt. Express* **13**(26), 10760–10767 (2005).
26. O. Pottiez, B. Ibarra-Escamilla, and E. A. Kuzin, "High-quality amplitude jitter reduction and extinction enhancement using a power-symmetric NOLM and a polarizer," *Opt. Express* **15**(5), 2564–2572 (2007).
27. J. Satsuma, and N. Yajima, "Initial value problems of one dimensional self-modulation of nonlinear waves in dispersive media," *Suppl. Prog. Theor. Phys.* **55**, 284–306 (1974).
28. G. P. Agrawal, *Nonlinear Fiber Optics* (Academic, San Diego, Ca., 2001).
29. B. Ibarra-Escamilla, O. Pottiez, E. A. Kuzin, M. Duran-Sanchez, and J. W. Haus, "All-fiber passive mode-locked laser to generate ps pulses based in a symmetrical NOLM," *Laser Phys.* **19**(2), 368–370 (2009).
30. R. Ulrich, and A. Simon, "Polarization optics of twisted single-mode fibers," *Appl. Opt.* **18**(13), 2241–2251 (1979).
31. E. A. Kuzin, J. M. Estudillo Ayala, B. Ibarra Escamilla, and J. W. Haus, "Measurements of beat length in short low-birefringence fibers," *Opt. Lett.* **26**(15), 1134–1136 (2001).
32. V. E. Zakharov, and A. B. Shabat, "Exact theory of twodimensional self-focusing and one-dimensional selfmodulation of waves in nonlinear media," *Sov. Phys. JETP* **61**, 62–69 (1972).
33. N. Korneev, E. A. Kuzin, B. Ibarra-Escamilla, M. Bello-Jiménez, and A. Flores-Rosas, "Initial development of supercontinuum in fibers with anomalous dispersion pumped by nanosecond-long pulses," *Opt. Express* **16**(4), 2636–2645 (2008).
34. O. Pottiez, E. A. Kuzin, B. Ibarra-Escamilla, and F. Méndez-Martínez, "Theoretical investigation of the NOLM with highly twisted fibre and a $\lambda/4$ birefringence bias," *Opt. Commun.* **254**(1-3), 152–167 (2005).
35. Y. Silberberg, and Y. Barad, "Rotating vector solitary waves in isotropic fibers," *Opt. Lett.* **20**(3), 246–248 (1995).
36. D. N. Payne, A. J. Barlow, and J. Hansen, "Development of low- and high-birefringence optical fibers," *IEEE J. Quantum Electron.* **QE-18**(4), 477–488 (1982).

1. Introduction

The nonlinear evolution of high-intensity optical pulses in optical fibers is a complex phenomenon that has attracted the attention of researchers for more than two decades. In this respect the nonlinear evolution in the region of anomalous group-velocity dispersion (GVD) is of special interest due to the ability to excite solitons as a result of the interplay between self-phase modulation (SPM) and anomalous GVD. This phenomenon was demonstrated by Mollenauer *et al.* for the first time in 1980. They reported the narrowing of picosecond (ps) pulses and the soliton generation in a fiber with anomalous GVD [1]. Later, very strong narrowing of ps pulses was demonstrated in [2,3]. The strong narrowing was associated with the periodic evolution of higher-order solitons. The inherent drawback of this pulse compression is that the quality of the compressed pulse is poor since it is located on a broad pedestal. At high power levels, higher order effects also play an important role in soliton formation. The most important among them is the soliton self-frequency shift (SSFS) [4,5]. It was shown that at the presence of SSFS high-order solitons decay into fundamental solitons

[6,7]. The fission of the high-order solitons was investigated in different nonlinear regimes and it was shown that it depends on the fiber dispersion, pulse duration, and chirp of the input pulse [8–12].

On the other hand, in cases involving continuous wave and relatively long pulse pumping, the effect of modulation instability (MI) seeds the formation of solitons by producing an exponential growth of small-amplitude perturbations [13]. This effect causes the breakup of the pump into short temporal pulses which in the presence of intrapulse Raman scattering, a phenomenon responsible for the SSFS, are shifted to lower frequencies forming fundamental solitons [14,15]. Numerical investigations show that pulse compression is the dominant effect at the initial stage of the soliton formation for pulses shorter than approximately 10 ps – 20 ps. For intermediate pulse durations the pulse compression is also observed, but at high noise power MI prevails. For the pulses longer than 100 ps the dominant effect is MI in seeding the formation of solitons [16]. An important characteristic of the soliton formation is that in cases involving high power levels the bound state of a high-order soliton no longer remains stable during propagation, and as a result the multisoliton pulse decays into fundamental solitons.

In the last decade the supercontinuum (SC) generation has received great attention after the demonstration of very wide optical spectra excited by intense optical pulses propagating in photonic crystal fibers. Since then, several schemes have been reported in which femto-, pico-, nano-second pulses and continuous wave were used for generating SC spectra [17–20]. MI, pulse breakup, soliton fission, SSFS, and four-wave mixing (FWM) are involved in the SC generation. Many investigations reported to date have been performed to understand in details the process of the SC formation, however because of the cascading effects and its sensitivity to experimental conditions a detailed comparison of experiment and theory is complicated. The investigations are commonly carried out using numerical simulations of the nonlinear Schrödinger equation (NLSE) and by measuring of the optical spectra.

The extraction of solitons with desirable pulse duration from a bunch of solitons could be useful for investigations of the soliton formation process and also for soliton generation. To the best of our knowledge, the experimental demonstration of the extraction of soliton from the bunch of solitons resulting from pulse breakup has not yet been reported. In this paper we experimentally investigate the soliton extraction from a bunch of solitons generated by 25-ps pulses in a fiber with anomalous dispersion. With the objective to obtain successful extraction, we consider the use of a nonlinear optical loop mirror (NOLM) whose capabilities for switching of solitons are already well-known [21–23]. In a previous work [24] we numerically demonstrated that the NOLM can be designed to obtain high transmission for solitons with specific duration, whereas solitons with shorter and longer durations are rejected. Moreover, the dependence of the NOLM transmission on the soliton duration can be shifted by amplification of the solitons before entering into the NOLM. This allows a selective transmission of solitons with specific duration that can be used for the extraction of a desired soliton.

In the proposed configuration we use a power symmetric NOLM which consist of a loop with highly twisted low-birefringence fiber, and a quarter-wave retarder (QWR) located asymmetrically in the loop that can be rotated in a plane perpendicular to the fiber to provide polarization asymmetry. In previous papers, this NOLM design has demonstrated high dynamic range, controllable transmission, and good stability during operation [25,26]. As a particular case we experimentally investigate the evolution of a 25-ps pulse with soliton number (N) in a range between 12 and 24. N is defined by the relation $N=(L_D/L_{NL})^{1/2}$, where $L_D=T_0^2/|\beta_2|$ and $L_{NL}=(\gamma P_0)^{-1}$ are the dispersion and nonlinear lengths of the pulse, respectively. T_0 is the half pulse duration at $1/e$ intensity point, β_2 is the GVD parameter (in ps²/km), γ is the nonlinear coefficient (in W⁻¹km⁻¹), and P_0 is the peak power of the incident pulse [27,28]. The pulse propagates through 500 m of the standard fiber with anomalous dispersion where the pulse breakup occurs and a bunch of fundamental solitons is formed. The resulting solitons are launched into the NOLM and the autocorrelation trace was

measured at the NOLM output. The experimental results demonstrate that the proposed configuration allows the extraction of a single soliton. For our particular case we report the extraction of a pulse with full width at half-maximum (FWHM) pulse duration (T_{FWHM}) of 1.46 ps, whose autocorrelation function closely corresponds to that of a soliton. Additionally, a standard fiber of 1 km is inserted at the NOLM output for pulse shaping applications. At the output we detect a soliton with T_{FWHM} of 0.99 ps. Our results demonstrate that the suggested method can be useful for soliton generation and also to investigate the initial stage of the soliton formation process.

2. Experimental setup

Figure 1 shows a schematic of the experimental setup. In this configuration initial pulses at 1550 nm were generated by a figure-eight fiber laser (F8L) described before in [29]. The F8L emits 25-ps pulses with peak power of ~1.2 W at a repetition rate of 0.8 MHz. The pulses have nearly Gaussian waveform and the pulse energy is estimated as 32 pJ. These pulses are amplified by an Erbium-doped fiber amplifier (EDFA-1) to achieve maximum peak power of ~20 W, and it is used to pump the Fiber 1. As the Fiber 1 we used 500-m SMF-28 twisted fiber with a twist rate of 5 turns per meter. The SMF-28 has anomalous dispersion equal to 20 ps/(nm-km) at 1550 nm. The twist in the fiber is manually introduced in order to eliminate the residual lineal birefringence, which is not controlled and can be changed with environmental conditions. The twist in the fiber induces a circular birefringence α proportional to the twist rate, $\alpha = g\tau$, where $g \approx 0.16$ for silica fibers [30] and the twist rate τ is measured in rad/m. At strong twist, the evolution of polarization is dominated by the induced circular birefringence. The value of the linear birefringence $\beta_{lin} = 2\pi/L_B = 0.4$ rad/m was obtained from the measured beat length of $L_B = 15.7$ m for the SMF-28 fiber [31]. At the twist rate of 5 turn/m the circular birefringence can be calculated as 5.03 rad/m. We verified experimentally that the twist rate of 7 turn/m as well as the 5 turn/m corresponds to the case of strong twist ($\alpha \gg \beta_{lin}$).

The resulting solitons coming from the Fiber 1 are amplified by a second Erbium-doped fiber amplifier (EDFA-2) to ensure that counterpropagating pulses in the NOLM loop have amplitude equal or higher than that of the corresponding soliton. The pulses amplified by the EDFA-2 pass through the polarization controller (PC) which is adjusted to obtain maximal transmission through the linear polarizer (LP). Then, the linear polarization is changed into a circular polarization state by the quarter-wave retarder (QWR2). The circular polarization is required for appropriate operation of the NOLM. Finally the pulses are launched into the NOLM made with 40-m SMF-28 fiber twisted with 7 turns per meter. The NOLM parameters are adjusted to transmit the highest power soliton.

Zakharov and Shabat [32] investigated the statistics of solitons resulting from the pulse breakup process. It can be expected from their results that the power of the highest soliton at the end of the process has to be approximately four times higher than the power of the input pump pulse. The model of the initial stage of supercontinuum generation, based on the results of Zakharov and Shabat, corroborates reasonable well with experimental results [33] the prediction of the model discussed in [32]. Thus, the highest soliton in our experiment is expected to be about 80 W corresponding to a T_{FWHM} of ~0.78 ps. A 1-km SMF-28 fiber (Fiber 2) is connected at the NOLM output for pulse shaping application.

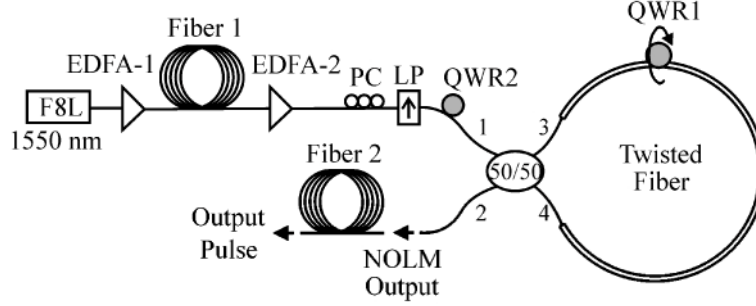


Fig. 1. Experimental setup used for the investigation of the soliton extraction.

One important property of this NOLM configuration is that the transmission can be easily modified through rotation of the QWR1. For the particular case of the circular input polarization the low-power transmission can be set to any value between 0 and 0.5 without changing the critical power (the power required for the phase shift of π between counterpropagating beams). It allows a very high contrast between high power and low power transmission [34]. At this length the NOLM exhibits a selective transmission that can be useful for the soliton extraction in a range between 0.4 and 1.87 ps. The EDFA-2 was made with a short, 3-m fiber with high Erbium concentration to avoid nonlinear and dispersion effects into the Erbium-doped fiber.

The operation of the NOLM for the soliton extraction can be described as follows. The resulting solitons coming from Fiber 1 are amplified, circularly polarized, and launched into the port 1 of the NOLM, where the symmetrical fiber coupler splits the beam into two beams of equal amplitude transmitted through the ports 3 and 4 to the NOLM loop. The coupler does not affect the polarization state, so the beam transmitted through port 3 is converted into a linearly polarized state by the QWR1 and propagates clockwise around the loop until it reaches the port 4. We modeled the linearly polarized beam as composed by the sum of two circularly polarized components and calculate its evolution using the circular polarization basis for our computations, see Eqs. (1). The counterclockwise beam propagates around the loop maintaining its initial circular polarization. We calculate its evolution with the same Eqs. (1) taking the initial condition $A_- = 0$. After passing through the QWR1 it converts its polarization state into linear and reaches the port 3. Finally linearly polarized beams are recombined in the coupler, and the differential nonlinear phase shift between counterpropagating beams determines if the pulse is transmitted or reflected. For calculations we used the coupled-wave equations in the following form [35]

$$\frac{\partial A_+}{\partial z} = \frac{\Delta\beta}{2} \frac{\partial A_+}{\partial T} + i \frac{\beta_2}{2} \frac{\partial^2 A_+}{\partial T^2} + i \frac{2}{3} \gamma (|A_+|^2 + 2|A_-|^2) A_+, \quad (1a)$$

$$\frac{\partial A_-}{\partial z} = -\frac{\Delta\beta}{2} \frac{\partial A_-}{\partial T} + i \frac{\beta_2}{2} \frac{\partial^2 A_-}{\partial T^2} + i \frac{2}{3} \gamma (|A_-|^2 + 2|A_+|^2) A_-, \quad (1b)$$

where A_+ and A_- represent the pulse envelope in the right- and left-circularly polarized states respectively; z represents the physical distance; the parameter $\Delta\beta$ represents the difference between the inverse of group velocities of the left- and right-circularly polarized components. This parameter is related to the twist rate through the relation $\Delta\beta = B_{cir}/c$, where c is the speed of light and the normalized circular birefringence B_{cir} is defined by the relation $B_{cir} = \lambda g \tau / 2\pi$ [36]. For the twist rates of 5 and 7 turns per meter $\Delta\beta$ is equal to 4.13 ps/km and 5.78 ps/km, respectively; β_2 is the GVD parameter equal to $-25.5 \text{ ps}^2/\text{km}$ that corresponds to a dispersion parameter D of 20 ps/(nm-km) at 1550 nm; T represents the physical time in the retarded frame, and γ is the nonlinear coefficient equal to $1.62 \text{ W}^{-1}\text{km}^{-1}$ obtained from the effective

area of $81 \mu\text{m}^2$ and the nonlinear coefficient $n_2=3.2 \times 10^{-20} \text{ m}^2/\text{W}$ for the SMF-28 fiber. Equations (1) are solved numerically with the split-step Fourier method. For the NOLM calculation we simplify our treatment by excluding the Raman term because its contribution is negligible for the short length of the NOLM loop.

Previously [24] we numerically demonstrated that the NOLM can be designed to obtain high transmission for solitons with specific duration, whereas solitons with shorter and longer durations are rejected. The range of soliton durations with high transmission depends on the NOLM loop length and can be shifted toward longer soliton durations by amplifying the solitons before entering into the NOLM. Figure 2 shows how the NOLM transmission depends on the soliton duration considering linearly polarized solitons at the end of Fiber 1. The simulation was made for the NOLM with the parameters used in the experiments, assuming the amplification of the EDFA-2 between 1.5 and 9.

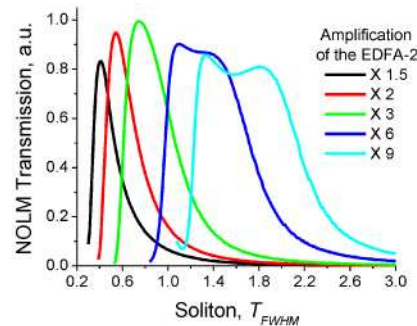


Fig. 2. NOLM transmission considering different amplification values of the EDFA-2.

As we can see, the dependence of the NOLM transmission on the soliton duration is very steep and can be changed just by adjusting the amplification of the EDFA-2. We can see that the maximum of the transmission shifts toward longer solitons as the amplification increases and the transmission drops abruptly for solitons with the duration shorter than some “critical” duration corresponding to maximal transmission. For the amplification of 1.5, the maximum transmission occurs for a soliton with duration of 0.40 ps, whereas for the amplification of 9 the maximum occurs for the soliton with duration of 1.33 ps. It should be noted that the best performance can be obtained with the amplification of the EDFA-2 between 2 and 3 times. These amplifications represent the special cases in which fundamental solitons with linear or circular polarization propagate in the loop. For the amplification of 2 times the clockwise pulse, after passing QWR1, has the power corresponding to the linearly polarized soliton, however the circular birefringence complicates the pulse evolution and it propagates almost like a soliton, while the counterclockwise pulse propagates with circular polarization and power lower than that corresponding to soliton ($N < 1$), undergoing dispersive effects. For the amplification equal to 3, the counterclockwise pulse propagates as a fundamental soliton with circular polarization, allowing complete transmission. The loop length (L) required for the maximum of the transmission is associated with the dispersion length L_D by the relation $L=5.7L_D$ [24]. In our case since we expect the formation of the highest solitons with duration of 0.78 ps, the loop length is chosen to be equal to 40 m allowing almost complete transmission for solitons around 0.78 ps.

3. Experimental results and discussion

When the pump pulse launched into Fiber 1 reaches a certain power level, it becomes unstable during propagation and breaks up temporally forming a bunch of individual soliton components. We investigate the soliton formation process using pump pulses in a range between 5 W to 20 W of peak power. Figure 3 shows the autocorrelation traces at the Fiber 1

output for 5 W, 9 W, and 20 W. The pulse energy of the pump pulses correspond to 133 pJ, 240 pJ, and 530 pJ, respectively.

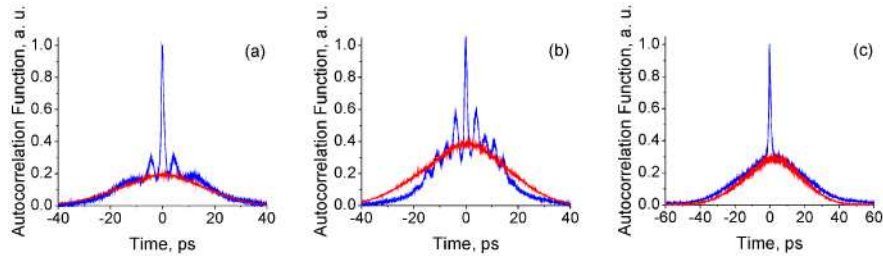


Fig. 3. Autocorrelation traces (blue line) at the Fiber 1 output at pump powers of: (a) 5 W, (b) 9 W, and (c) 20 W. The red line corresponds to the autocorrelation function of the input pulse.

It has to be taken into account that each autocorrelation trace represents an average of many autocorrelation traces. Figure 3(a) represents the initial stage of the breakup with a small number of high power peaks. As the pump power increases (Fig. 3(b)), the number of high power peaks increases. However the pulse waveform is well defined and similar for all pulses. It allows the detection of peaks in the averaged autocorrelation trace. Some compression of the pulse envelope can be seen in the Fig. 3(b). Finally at higher power, Fig. 3(c), the averaged autocorrelation trace does not reveal the multiple peaks which mean that each pulse forms a random soliton bunch. Figure 3(c) shows also the broadening of the autocorrelation trace caused probably by the soliton self-frequency shift and the displacement of the solitons with respect to the envelope. Below we show the extraction of a single soliton for the cases corresponding to the Figs. 3(a)-(c).

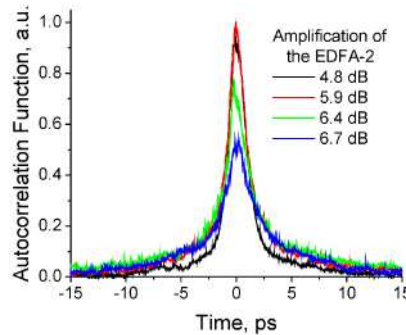


Fig. 4. Autocorrelation traces at the NOLM output at different amplifications of the EDFA-2.

Figure 4 shows the autocorrelation traces at the NOLM output for different amplifications of the EDFA-2. The amplifications of 4.8 dB and 5.9 dB provide the transmission close to its maximum value. Higher amplification results in fast decrease of the transmission due to the shift of the transmission maximum toward longer solitons, see Fig. 2. The quantitative comparison between the calculated dependencies in Fig. 2 and experimental results presents difficulties because of loss in the polarizer that are not well known. Using continuous wave light the polarizer loss is measured as 1.2 dB, however in the case of pulses the polarizer loss increases up to 3.1 dB. We believe that this behavior is due to the small nonlinear polarization rotation. We tried to use linear polarization to avoid this effect, however even small ellipticity of the polarization may cause the nonlinear polarization rotation. Pulses with different power undergo different nonlinear polarization rotation, and as a result the polarizer losses in experiment are not well defined. In experiments we adjusted the best amplification observing the autocorrelation traces at the NOLM output. Figure 5 shows the autocorrelation traces corresponding to the soliton extraction for the three characteristic stages of the pulse breakup

shown in Figs. 3(a)-(c). For these cases the amplification of the EDFA-2 was about 6.4 dB. In the NOLM the QWR1 is adjusted to have zero low-power transmission of the NOLM.

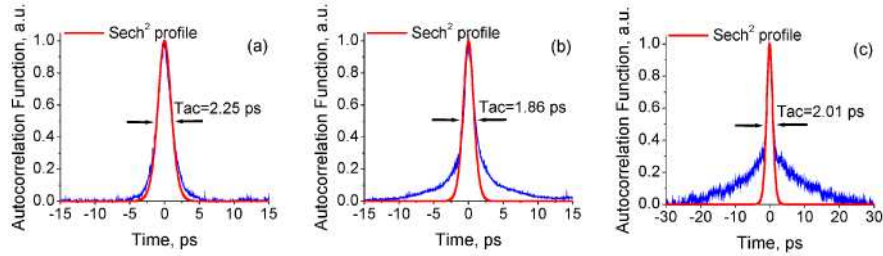


Fig. 5. Autocorrelation traces at the NOLM output corresponding to the cases shown in Fig. 3(a), Fig. 3(b), and Fig. 3(c) respectively.

It is interesting to note that at the initial stage of the pulse breakup (Fig. 3(a)) successful extraction of a single soliton is achieved (Fig. 5(a)). We believe that this is possible due the fact that the soliton bunch at the end of Fiber 1 consists of a small number of solitons with high ratio between the amplitude of the strongest and the next pulse. As a result, it is relatively easily to adjust the NOLM transmission for the extraction of a single soliton. From this result a T_{FWHM} of 1.46 ps is estimated from the FWHM duration of the autocorrelation trace (Tac) of 2.25 ps ($T_{FWHM}=0.648\text{Tac}$). The average power at the NOLM output was 0.05 mW. Assuming that there are not dispersive waves at the NOLM output, we can estimate the pulse energy using the measured average power and the frequency repetition rate to be equal to 62.5 pJ. The maximum peak power is estimated as 37.8 W and the soliton number N is estimated as 1.3. Indeed as it will be shown below the fraction of the dispersive waves is only 10% of the power. For the case shown in Fig. 5(b) the situation differs due to the increase of the number of solitons. Solitons with duration slightly longer than that of the highest soliton appear and the transmission of a single soliton is more complicate since the NOLM allows the transmission of solitons whose duration is slightly longer than that of the highest soliton, see Fig. 2. For this case the T_{FWHM} is estimated as 1.21 ps from the autocorrelation trace duration of 1.86 ps. This value represents a rough estimation since not exactly sech^2 profile is observed. For the case shown in Fig. 5(c) the autocorrelation trace is similar to that shown in Fig. 5(b). The T_{FWHM} of the transmitted pulse is estimated as 1.3 ps from the autocorrelation value of 2.01 ps. For the cases shown in the Fig. 5(b) and Fig. 5(c) the extracted pulses are accompanied by low-power pulses, therefore it is not possible to obtain an appropriate estimation of the peak power and consequently the soliton number and the pulse energy.

One of the interesting features of this NOLM configuration is the possibility to adjust the low-power transmission by the QWR1 rotation. We can adjust the QWR1 angle in such a manner that the transmission for low power has some value between 0 and 0.5. Figure 6(a) shows two calculated nonlinear transmissions of the NOLM considering two different angles of the QWR1. The red line shows the case in which QWR1 is adjusted to have zero low-power transmission. In experiments we obtained a transmission of -32 dB for the low-intensity components. The blue line shows the transmission when the QWR1 is rotated by 10 degrees. At this QWR1 angle an increase of the power firstly results in the drop of the transmission reaching zero and then begins to increase. This dependence allows the rejection of respectively high power input pulses. Figure 6(b) and Fig. 6(c) show the autocorrelation traces at the NOLM output for the cases discussed in Fig. 5(b) and Fig. 5(c) considering the rotation of the QWR1 by approximately 10 degrees with respect to the angle of zero low-power transmission. As we can see, in both cases we reached the reducing of low-power components by approximately 2 – 3 times. The transmitted pulses in Fig. 6(b) and Fig. 6(c) have T_{FWHM} of 0.91 ps and 0.87 ps respectively.

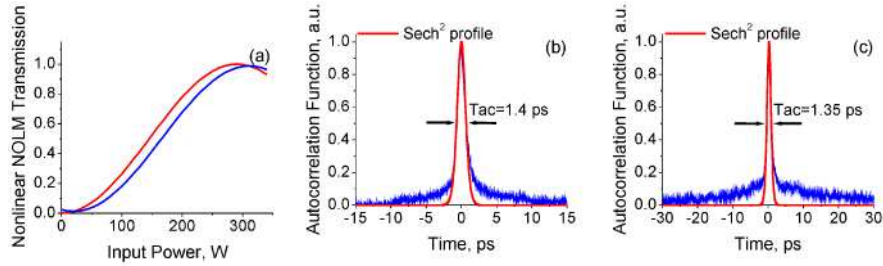


Fig. 6. (a) Nonlinear NOLM transmission considering two different angles of the QWR1; Autocorrelation traces at the NOLM output considering a QWR1 angle of 10 degrees with respect to the angle of zero low-power transmission for the cases discussed in Fig. 5(b) and Fig. 5(c) respectively.

One way to obtain fundamental solitons is to use the pulse evolution in a nonlinear dispersive medium. For low-intensity pulses ($N < 1$) dispersion effects dominate and give rise to pulse broadening, whereas for pulses with higher soliton number ($N > 1$) the nonlinearity dominates, and the pulse experiences a narrowing effect defined by the input power. Besides, it has also been demonstrated that if the pulse does not correspond exactly to an optical soliton for N in the range between 0.5 and 1.5, the pulse adjusts its shape and width as it propagates along the fiber and evolves into a fundamental soliton [27,28]. We launched the pulse from the NOLM output into the 1-km SMF-28 fiber (Fiber 2) used as nonlinear dispersive medium. Figure 7 shows the autocorrelation trace at the Fiber 2 output considering as the Fiber 2 input the 1.46 ps pulse at the NOLM output shown in Fig. 5(a). For this case, the length of Fiber 2 corresponds to 37 times the dispersion length for the 1.46 ps pulse.

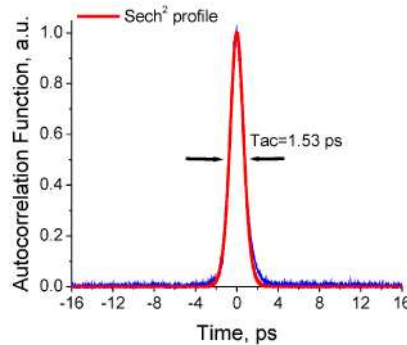


Fig. 7. Autocorrelation trace at the output of the 1 Km fiber.

The T_{FWHM} for this pulse is estimated as 0.99 ps. The peak power for the 0.99 ps soliton can be calculated using the fiber parameters as 50 W and the pulse energy is calculated as 56 pJ. If we calculate the pulse energy as the average power divided by the repetition frequency, the pulse energy at the Fiber 2 input will be found as 62.5 pJ. The difference in energy appears because of the dispersive waves increasing average power. From these data we can conclude that 90% of the power at the Fiber 2 output is in form of a soliton, and only 10% is in form of dispersive waves. The total average power at the Fiber 2 output is 0.05 mW. Thus, the average power of the dispersive waves can be estimated as 5 μ W and the contrast between the soliton peak power and average power of dispersive waves is 70 dB. For the case of Fig. 7 we have measured the energy at the NOLM input equal to 350 pJ. Respectively the ratio between the energy of the 0.99-ps soliton and the energy of the pulse at the NOLM input is 0.16. This value can be considered as part of the input energy corresponding to the highest soliton in the bunch of solitons.

4. Conclusions

We experimentally investigated the transmission of a bunch of solitons resulting from pulse breakup through a NOLM and found that under some conditions a fundamental soliton can be extracted. For our particular case, we used 25-ps pulses with the corresponding soliton number N in a range between 12 and 24 to generate a soliton bunch in the 500-m standard fiber. Then we used our NOLM proposed earlier to extract a single soliton from the bunch. The experimental results demonstrate that with the proposed configuration the extraction of individual soliton can be done. We observed the transmission of the highest soliton through the NOLM and strong rejection of solitons with lower power. The contrast between the soliton power and average power of dispersive was estimated as 70 dB with only 10% of the dispersive wave fraction in the total power. Our results demonstrate that the suggested method can be useful for soliton generation and also for investigations of the initial stage of the soliton formation process.